Reproduction of Reflective and Fluorescent Components using Eight-band Imaging

M. Tsuchida, M. Mori, K. Kashino, and J. Yamato
NTT Communication Science Laboratories / 3-1 Morinosato-Wakamiya, Atsugi-shi, Kanagawa, JAPAN

Abstract

We propose a method for relighting fluorescent objects using a multiband image system. Fluorescence is often present in everyday articles and its optical properties make it harder to reproduce than pure reflectance. Decomposing colors into separate fluorescent and reflective components is required for accurate color reproduction. In our method, bi-spectral images are captured using an eight-band camera and an eight-band lighting system for the decomposition. First, spectral reflectance of the object is estimated. Next, the multiband image of the fluorescent components under relighting illumination is generated from the weighted linear combination of the captured fluorescent images. The weight of each band is calculated from the spectral transmittance of each band-pass filter attached to the lighting system, and the spectral power distributions (SPD) of the illumination during image capturing and relighting. Finally, a relighted image is reproduced by composing reflective and fluorescent component images. Experimental evaluations show that the spectral reflectance and SPD of fluorescent components are accurately estimated and relighting images are well reproduced.

Introduction

Reproduction of a material's appearance in an image is very important for perceiving the reality of an object. To realize this purpose, improving some factors such as image resolution, texture, gloss and three-dimensional effect is required. Color is also one of the important components. Which colors are observed depends on the spectral power distribution (SPD) of incident light and the optical properties at each point on the object's surface. In general, only spectral reflectance has been considered as the relevant optical property. However, analyzing the SPDs of lights from an object's surface often shows that reflective and fluorescent components are mixed. Fluorescence exists in everyday articles such as paper, package, cloth, flower and food. Fluorescence occurs not only in artificial materials but also in natural objects. The optical properties of reflection and fluorescence are quite different, and this requires the decomposition and analysis of each component for accurate color reproduction of a target object.

Accurate color reproduction of an object under arbitrary illuminative conditions is difficult when current imaging systems based on three-channels (i.e. Red, Green, and Blue) are used for image capturing. Multispectral imaging technology, which estimates the spectrum of an object using multiband data, provides accurate color reproduction. Several types of multiband camera systems [1-9] and a multiband imaging system using multiband lighting system have been developed [10]. These methods are effective for estimating spectral reflectance; however, the SPD of fluorescent components cannot be estimated.

Several methods for estimating the SPD of fluorescent components have also been developed using a hyperspectral camera (the number of color channels is more than sixteen) and visible light. In conventional methods, all combinations of incident and observed light wavelengths are examined, which is not practical for imaging systems. Tominaga et al. capture hyperspectral images under two kinds of illumination [11]. The feature of this method is to use ordinary illuminations, which overcomes the limitations of the lighting condition and size of the target objects. Fu et al. have developed a system wherein a hyperspectral camera and a programmable light source are combined and model parameters of fluorescence (absorption and emission spectra) are estimated [12]. In their method, high-frequency illuminations in the spectral domain are generated and only two hyperspectral images are captured.

Hyperspectral cameras have higher spectral resolution than most multiband cameras and can obtain relatively accurate spectra. However, higher sensitivity of each color channel is required because the narrowness of the bandwidth at each color channel reduces the power of incident light on the image sensor. And programmable light source is also required for analyzing fluorescence. These systems are still quite costly.

In this paper, we propose a method for decomposing reflective and fluorescent components, and generating an image relighted by an illumination that is different from that of the image-capturing environment. Our imaging system consists of an eight-band camera and an eight-band lighting system. The filter sets used in both systems are the same. Our method comprises four steps: capturing images, generating relighted reflective image, generating relighted fluorescent image, and combining the reflective and fluorescent images. Thirty-six images are captured and used for the decomposition. Eight images are used for reproducing the reflective image. The weighted linear combination of the remaining twenty-eight images is used for generating the relighted fluorescent image. The weights are calculated using the spectral transmittance of the filters and the SPDs of the illuminations for both image capturing and relighting. This approach is based on the phenomenon that the SPD of fluorescence depends on the energy of incident light. The feasibility of the proposed method is shown through experimental results. Materials used in the experiments were color patches and woven cloth on Japanese dolls.

Reproduction of Reflective and Fluorescent Components

Modeling and decomposition of reflective and fluorescent components

Let us consider the case where 1) a multiband image is captured using an *N*-band camera and *N*-band lighting system, 2)

the same set of band-pass filters is used in both systems, and 3) there is no overlap of spectral transmittance between each band-pass filter. When an object under the j th band illumination is captured by the i th band sensor ($1 \le i, j \le N$), the output signal of the reflective component is described as

$$r_{i,j} = \int_{380}^{780} I(\lambda) T_j(\lambda) R(\lambda) S_i(\lambda) d\lambda \quad (\text{when } i = j)$$
$$= 0 \quad (\text{when } i \neq j), \tag{1}$$

where λ is the wavelength, $I(\lambda)$ is the SPD of illumination, $T_j(\lambda)$ is the spectral transmittance of the filter, $R(\lambda)$ is the spectral reflectance of the object's surface, and $S_i(\lambda)$ is the spectral sensitivity. Then, the N-band image of the reflective component is obtained as

$$r_i = \int_{380}^{780} I(\lambda) T_i(\lambda) R(\lambda) S_i(\lambda) d\lambda \,. \tag{2}$$

On the other hand, fluorescence has a different optical property. An incident light at shorter wavelength is absorbed and its energy is emitted at longer wavelength. The output signal of the fluorescent component is described as

$$f_{i,j} = \int_{380}^{780} \left(\int_{380}^{780} I(\lambda') T_j(\lambda') \alpha(\lambda') d\lambda' \right) E(\lambda) S_i(\lambda) d\lambda$$
$$= \left(\int_{380}^{780} I(\lambda') T_j(\lambda') \alpha(\lambda') d\lambda' \right) \int_{380}^{780} E(\lambda) S_i(\lambda) d\lambda \ (\text{when } j < i)$$
$$= 0 \quad (\text{when } j > i), \tag{3}$$

where $\alpha(\lambda)$ and $E(\lambda)$ are the absorption and emission spectra. The N-band image of the fluorescent component is obtained according to eqs. (3) and

$$f_i = \sum_{j=1}^{i-1} f_{i,j} \quad (1 \le i \le N), \tag{4}$$

Relighting of fluorescent component

If the bandwidth of $T_j(\lambda)$ is small enough, $\alpha(\lambda)$ can be regarded as constant and eq. (3) can be rewritten as

$$f_{i,j} = k_j \left(\int_{380}^{780} I(\lambda') T_j(\lambda') d\lambda' \right) \int_{380}^{780} E(\lambda) S_i(\lambda) d\lambda \,, \tag{5}$$

when $j < i$. The second term of eq. (5) represents the energy of the j th band illumination, and it can be measured using a spectroradiometer. Relighting of the fluorescent component is conducted using this property.

Let us consider that the object is relighted by an illumination whose SPD is $I'(\lambda)$. The image of fluorescent component under illumination $I'(\lambda)$ can be described using eq. (5) as

$$f'_{i,j} = k_j \left(\int_{380}^{780} I'(\lambda') T_j(\lambda') d\lambda' \right) \int_{380}^{780} E(\lambda) S_i(\lambda) d\lambda$$
$$= \frac{\int_{380}^{780} I'(\lambda') T_j(\lambda') d\lambda'}{\int_{380}^{780} I(\lambda') T_j(\lambda') d\lambda'} f_{i,j} \,, \tag{6}$$

and the relighted N-band image of the fluorescent component can be generated from the weighted linear combination of the captured images as

$$f'_i = \sum_{j=1}^{i-1} \{ w_j \cdot f_{i,j} \} \,, \tag{7}$$

$$w_j = \int_{380}^{780} I'(\lambda') T_j(\lambda') d\lambda' \Big/ \int_{380}^{780} I(\lambda') T_j(\lambda') d\lambda' \,, \tag{8}$$

The weight of each band is calculated using the spectral transmittance of the filters and the SPDs of the illuminations for both image capturing and relighting as eq. (8).

Spectral estimation from multiband image

Some methods for estimating spectral reflectance from multiband data have been proposed, all of which can be applied to our method. Here, the Wiener estimation method [13] is introduced as one of the simplest methods.

Let the spectral sensitivity of the sensor be $\mathbf{S} = [S_1(\lambda), S_2(\lambda), \cdots, S_N(\lambda)]^T$. Let the matrix whose diagonal elements represent the SPD of illumination be $\mathbf{I}$. The observed spectrum is described as

$$\mathbf{s}_r = \mathbf{IR} \tag{9}$$

The spectral reflectance, $\mathbf{R}$, is estimated from the sensor output signal, $\mathbf{r} = \mathbf{SIR} = \mathbf{HR}$, as

$$\hat{\mathbf{R}} = \mathbf{Mr} \,, \qquad \mathbf{M} = \mathbf{KH}^t \{ \mathbf{HKH}^t \}^{-1} \,, \tag{10}$$

where $\hat{\mathbf{R}}$ is the estimated spectral reflectance, $\mathbf{M}$ is the Wiener estimation matrix, and $\mathbf{K}$ is a priori knowledge about spectral reflectance of the object. Here, we use a correlation matrix, $\mathbf{K}$, which is modeled on a first-order Markov process covariance matrix, represented as

$$\mathbf{K} = \begin{pmatrix} 1 & \rho & \rho^2 & \cdots & \rho^{N-1} \\ \rho & 1 & \rho & \cdots & \rho^{N-2} \\ \rho^2 & \rho & 1 & \cdots & \cdots \\ \cdots & \cdots & \cdots & \cdots & \cdots \\ \rho^{N-1} & \rho^{N-2} & \cdots & \cdots & 1 \end{pmatrix}, \tag{11}$$

where ρ is the adjacent element correlation factor. We set ρ to 0.999 in our experiments.

Using the estimated spectral reflectance and the SPD of illumination for relighting $\tilde{\mathbf{I}}$, the spectrum of the reflective component is calculated as $\hat{\mathbf{s}}_r = \tilde{\mathbf{I}} \hat{\mathbf{R}}$. The same procedure can be applied to estimate the SPD of fluorescent component $\hat{\mathbf{E}}$. In this case, the diagonal elements of matrix $\mathbf{I}'$ are 1.

$$\hat{\mathbf{E}} = \mathbf{M}' \mathbf{f}' \,, \tag{12}$$

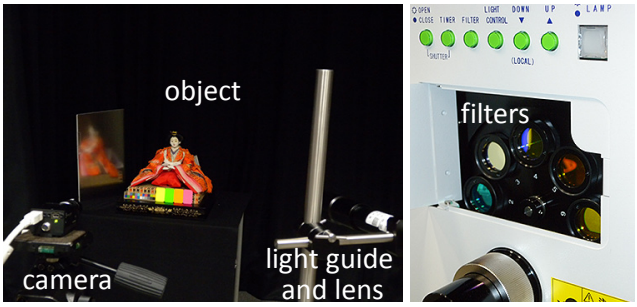

Figure 1. Experimental setup.
Layout of the equipment (left) and lighting system (right).

where $\mathbf{f}'=[f'_1, f'_2, \cdots, f'_N]^T$, $\mathbf{M}'=\mathbf{KH}'^t\{\mathbf{H}'\mathbf{KH}'^t\}^{-1}$, and $\mathbf{H}'=\mathbf{SI}'$. Then, the spectrum after relighting can be described as

$$\mathbf{s}=\tilde{\mathbf{I}}\hat{\mathbf{R}}+\hat{\mathbf{E}}. \quad (13)$$

Output RGB signals are calculated using the color matching function, and the tone curves and chromaticity values of primary colors of the display monitor.

Experiments

Experimental setup

Figure 1 shows the experimental setup. Images were captured with a monochrome CCD camera (GRAS-20S4M, Point Grey Research inc.). The camera can write out raw image data without any color correction and can take UXGA-size (1600 × 1200 pixels) images, each of which has bit-depth of 16 bits. The eight-band lighting system (LAX-103, Asahi spectra) consists of an xenon lamp and a filter turret. Band-pass filters for the camera are changed by hand, whereas filters of the lighting system can be controlled by software on a computer. The center wavelengths of the band-pass filters are 420, 450, 490, 530, 570, 610, 650, and 690 nm. The full width at half maximum (FWHM) of the first filter is 20 nm; the FWHM of the others is 40 nm. Figure 2 shows the total spectral sensitivity of the camera system and SPDs of the lighting system. As a target objects, reflective color chart (handmade small Macbeth color checker), fluorescent color cards, and woven clothes on Japanese dolls were used.

Figure 3 shows an example of captured images. The total number of images is thirty-six. The exposure time and aperture value of lens were fixed during image capturing. Focus was adjusted for each band of illumination. In addition, alignment errors among captured images caused by camera movement and optical aberration of the lens were corrected by image transformation using detected correspondences.

Visual evaluation of decomposition

The shows results of decomposing reflective and fluorescent components are shown in Fig. 4, where (a) and (d) are color reproduction images from the eight-band image, (b) and (e) are estimated reflective component images, and (c) and (f) are estimated fluorescent component images. Comparison with the reflective color chart indicates that the color of the reflective component was well reproduced. For fluorescent color cards and

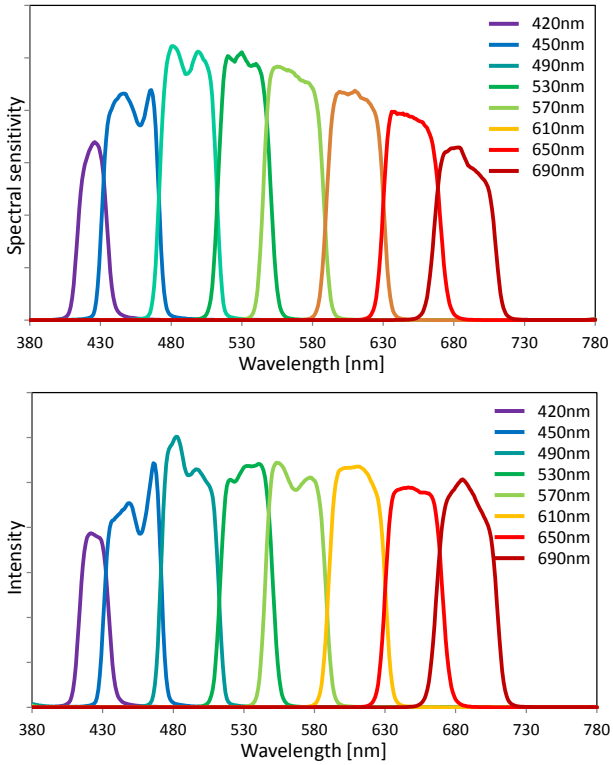

Figure 2. Total spectral sensitivity of camera (top) and SPDs of lighting system (bottom).

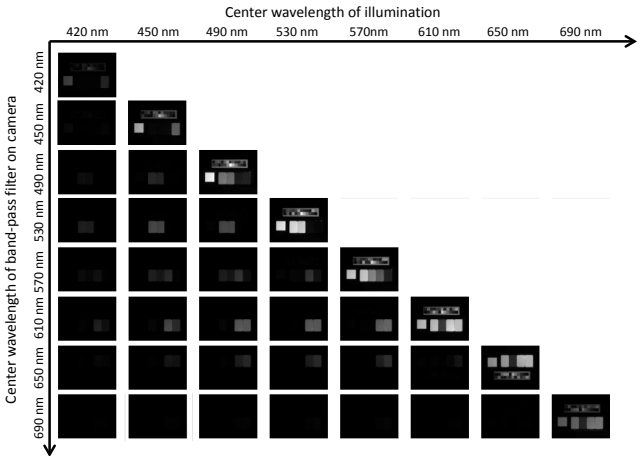

Figure 3. Example of captured images

reddish part of the woven clothes, reflective and fluorescent components seem to be well separated. When both component images were summed, the resultant images look almost the same as shown in (a) and (d).

Spectral and chromatic evaluations of decomposition

Figure 5 shows estimation results of the fluorescent component of color cards. SPDs of fluorescence are plotted on each graph, and their intensities were normalized by those of standard white. Estimated results were compared with measured data. For yellow

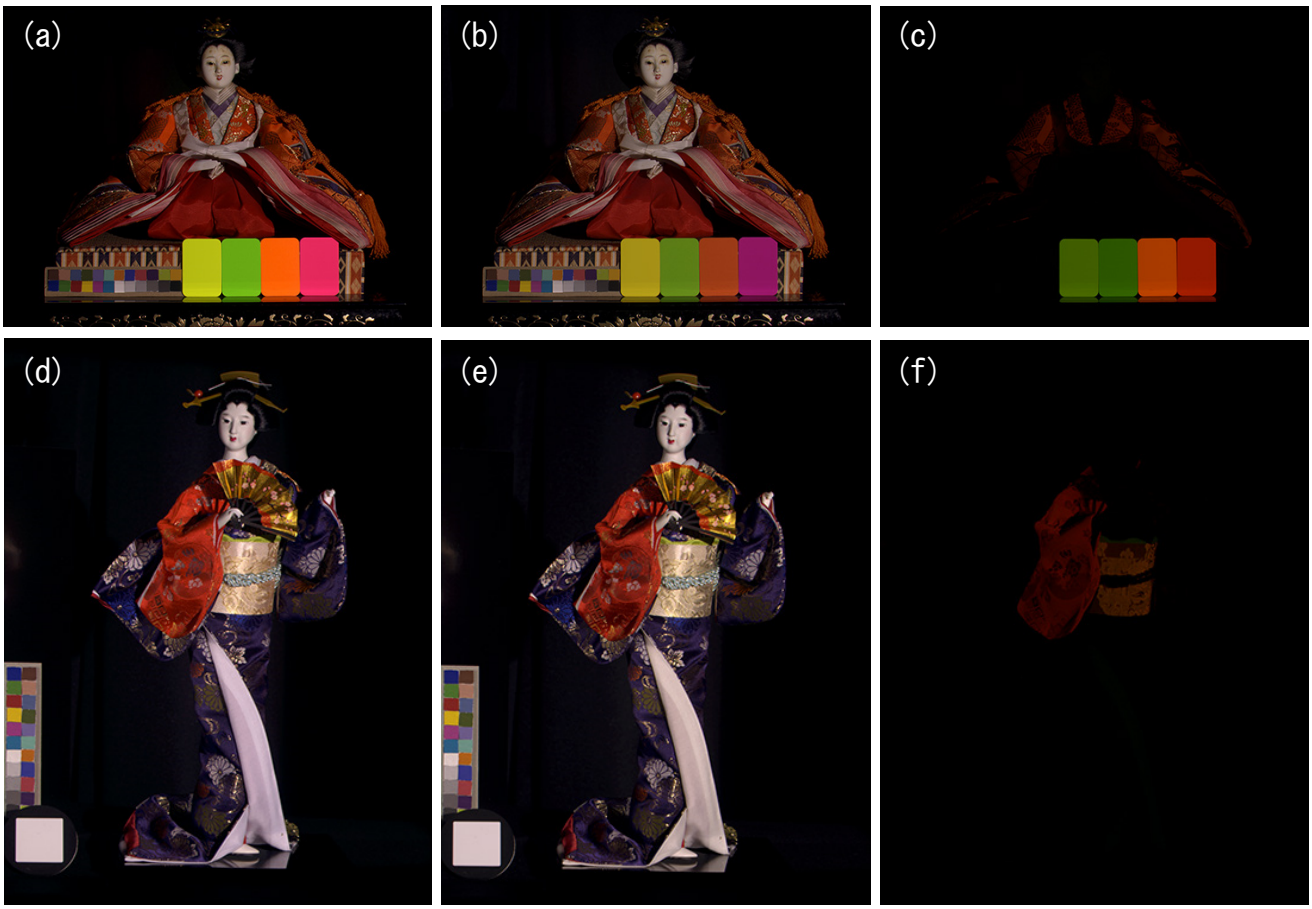

Figure.4. Results of decomposing reflective and fluorescent components.
(a) (d) : Color reproduction images from eight-band image. (b) (e): Reflective component, (c) (d): fluorescent component.

and green, the FWHM was well reproduced, but the wavelength at the peak was shifted approximately 15 nm. For orange and pink, the wavelength at the peak was shifted approximately 5 nm, but the FWHM was widened approximately 10 nm. In addition, relatively larger error tended to occur in the band of wavelengths longer than 680 nm cause of a lack of spectral data at this band and the use of the Wiener estimation based on a first-order Markov process model. Next, chromaticity values of measured and estimated spectra were calculated and plotted on a CIE-u'v' chromaticity diagram (see Fig. 6). Squares represent measured data and diamonds represent estimated results. These results show that colors of fluorescent components were well estimated with only a little error in spectral shape.

Relighting results

Captured multiband images were relighted by a fluorescent lamp and an incandescent lamp, according to the algorithm proposed in this paper. SPDs of both lamps are shown in Fig. 7. The SPD of the xenon lamp used in the multiband lighting system is also plotted on the graph as a reference. The fluorescent lamp has a spiky SPD and the incandescent lamp has a smooth one.

First, estimated spectra of fluorescent cards were compared with measured spectra in both illuminative conditions (see Figs. 8 and 9). For relighting by the fluorescent lamp, estimated spectra

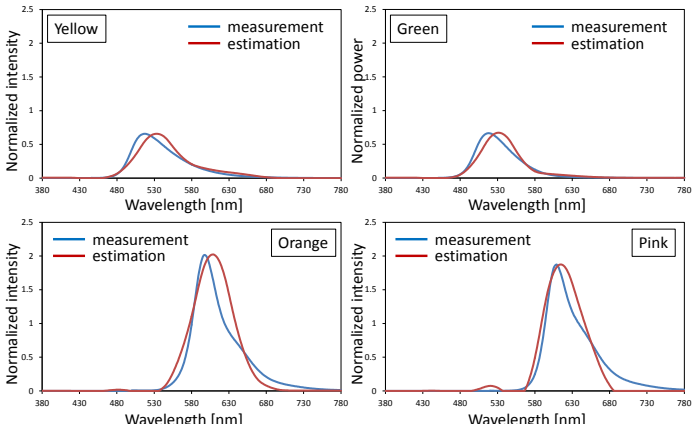

Figure 5. SPDs of fluorescent component.

were well fitted to the measured one even where spiky peaks existed. On the other hand, estimation errors were found for relighting by the incandescent lamp, especially for the orange card. This was caused by estimation error of the fluorescent spectrum, and errors in the band of wavelength longer than 680 nm also existed.

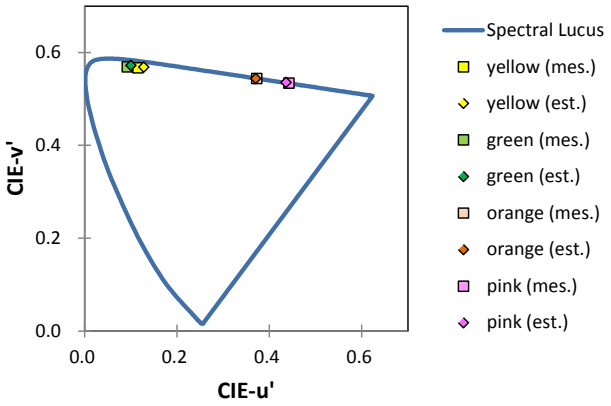

Figure 6. Chromaticity diagram plotting color of fluorescent component.

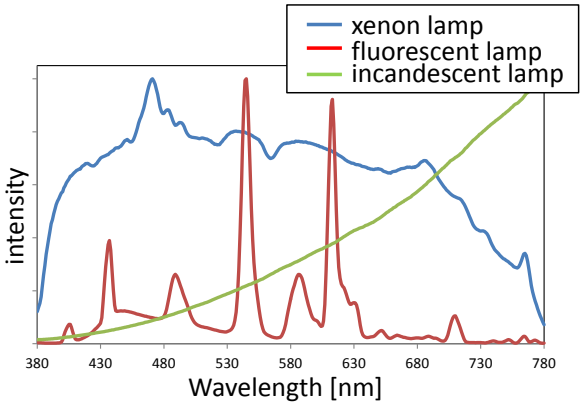

Figure 7. SPDs of illuminations used in relighting experiments.

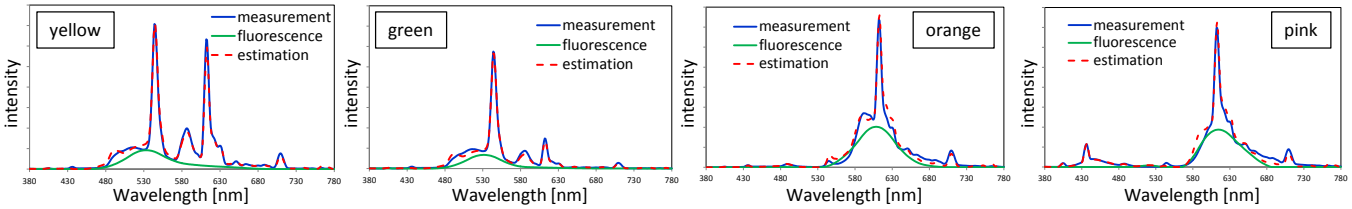

Figure 8. Spectra of fluorescent color cards relighted by fluorescent lamp.

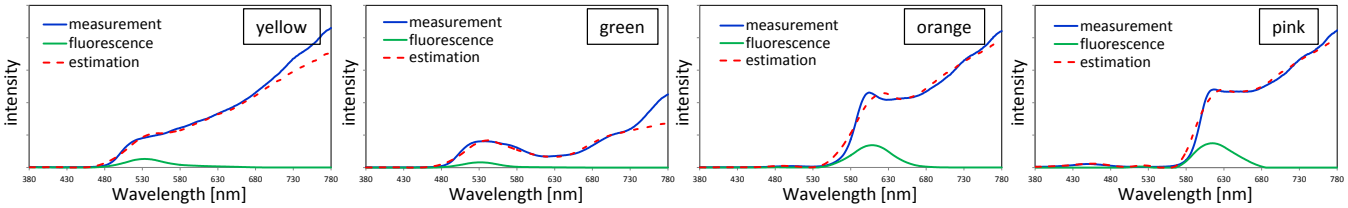

Figure 9. Spectra of fluorescent color cards relighted by incandescent lamp.

Next, relighted images and images captured under the actual illumination were compared. Figure 10 shows the resultant relighted images. Although the brightness of the orange card was not sufficient, the color and material appearance of the woven clothes were well reproduced.

Conclusion

We propose a method for decomposing reflective and fluorescent component, and generating an image relighted by an illumination that is different from that in the image-capturing environment. The method uses multiband imaging technology instead of hyperspectral imaging, and operations in the spectral domain are not necessary. Experiments were conducted using eight-band imaging systems. Experimental results show that decomposition of reflective and fluorescent component, and relighting were a successful, confirming the effectiveness of our method. For multiband image capturing in this work, band-pass filters for the camera were changed by hand, whereas filters for the lighting system were controlled by computer. The camera system can be replaced with a stereo multiband camera system [8] that can take an eight-band image with one-shot. Our next step is to conduct experiments using the stereo camera system.

References

[1] P.D. Burns and R.S. Berns, "Analysis of multispectral image capture." Proc. CIC4, pp. 19-22, 1996.

[2] S. Tominaga, "Multichannel vision system for estimating surface and illuminant functions." J. Opt. Soc. Am. A, 13(11), pp. 2163-2173, 1996.

[3] S. Tominaga et al., "Object Recognition by Multi-Spectral Imaging with a Liquid Crystal Filter.", Proc. ICPR, vol.1, pp. 708-711, 2000.

[4] K. Ohsawa et al., "Six-band HDTV camera system for spectrum-based color reproduction.", J. of Imaging Science and Technology, 48, 2, pp. 85-92, 2004.

Figure 10. Images relighted by fluorescent lamp and incandescent lamp.

[5] M. Hashimoto, et al., “Two-Shot type 6-band still image capturing system using Commercial Digital Camera and Custom Color Filter.”, Proc. CGIV, 538-541, 2008.

[6] M. Tsuchida et al., “A stereo one-shot multi-band camera system for accurate color reproduction.”, Proc. ACM SIGGRAPH, Poster (article No. 66), 2010.

[7] R. Shrestha et al., “One-shot multispectral color imaging with a stereo camera.”, Proc. SPIE, vol.7876, 797609-1 - 797609-11, 2011.

[8] M. Tsuchida et al., “A stereo nine-band camera for accurate color and spectrum reproduction”, Proc. ACM SIGGRAPH, Poster (Article No. 18), 2012.

[9] Y. Murakami et al., “Hybrid-resolution multispectral imaging based on color filter array: Basic principles and computer simulation”, Proc. CGIV, 259-265, 2012.

[10] J-I. Park, et al, “Multispectral Imaging Using Multiplexed Illumination.”, Proc. ICCV, 1-8, 2007.

[11] S. Tominaga, et al., “Spectral Estimation of Fluorescent Objects Using Visible Lights and an Imaging Device.”, Proc. CIC19, 352-356, 2011

[12] Y. Fu, et al., "Separating Reflective and Fluorescent Components Using High Frequency llumination in the Spectral Domain", Proc. ICCV, 457-464, 2013.

[13] W. K. Pratt, et al., “Spectral estimation techniques for the spectral calibration of a color image scanner.”, Applied Optics, 15, 73–75, 1976.

Author Biography

Masaru Tsuchida received the B.E., M.E. and Ph.D. degrees from the Tokyo Institute of Technology, Tokyo, in 1997, 1999, 2002, respectively. In 2002, he joined NTT Communication Science Laboratories, where his research areas included color science, three-dimensional image processing, and computer vision. His specialty is color measurement and multiband image processing. From 2003 to 2006, he worked as a researcher at the National Institute of Information and Communication Technology (NICT) for the "Natural Vision" project.